Deep groundwater flow and geochemical processes in limestone aquifers: evidence from thermal waters in Derbyshire, England, UK

John Gunn · Simon H. Bottrell · David J. Lowe · Stephen R. H. Worthington

Abstract Thermal waters potentially provide information on geochemical processes acting deep within aquifers. New isotopic data on groundwater sulphate, inorganic carbon and strontium in thermal and non-thermal waters of a major limestone aquifer system in Derbyshire, England, UK, are used to constrain sulphate sources and groundwater evolution. Shallow groundwaters gain sulphate from oxidation of sulphide minerals and have relatively ^{13}C-depleted dissolved inorganic carbon (DIC). Thermal waters have relatively high Sr/Ca and more ^{13}C-enriched DIC as a result of increased water–rock interaction. In other respects, the thermal waters define two distinct groups. Thermal waters rising at Buxton have higher Mg, Mn and $^{87}Sr/^{86}Sr$ and lower Ca and SO_4, indicating flow from deep sandstone aquifers via a high permeability pathway in the limestone. By contrast, Matlock-type waters (97% of the thermal flux) have elevated sulphate concentrations derived from interaction with buried evaporites, with no chemical evidence for flow below the limestone. About 5% of the limestone area's groundwater flows to the Matlock group springs via deep regional flow and the remainder flows via local shallow paths to many non-thermal springs. Gypsum dissolution has produced significant tertiary porosity and tertiary permeability in the carbonate aquifer and this is an essential precursor to the development of karstic drainage.

Résumé Les eaux thermales peuvent apporter des informations sur les processus géochimiques dans les aquifères profonds. De nouvelles données isotopiques sur les sulfates présents dans les eaux souterraines, le carbone inorganique et le strontium dans les eaux thermales et non thermales d'un système aquifère calcaire majeur dans le Derbyshire, Angleterre, Royaume Uni, sont utilisées pour comprendre les sources de sulfates et l'évolution des eaux souterraines. Les eaux souterraines phréatique s'enrichissent en sulfate via l'oxydation des minéraux sulfatés et ont un Carbone Inorganique Dissous (DIC) relativement appauvri en ^{13}C. Les eaux thermales ont un rapport Sr/Ca relativement plus élevé et un DIC plus enrichi en ^{13}C, du fait de l'interaction accrue des eaux avec les roches. En d'autres mots, les eaux thermales définissent deux groupes distincts. Les eaux thermales remontant à Buxton ont un Mg, un Mn et un rapport $^{87}Sr/^{86}Sr$ plus hauts, mais un Ca et SO_4 plus faible, indiquant un écoulement à travers les zones perméables des aquifers gréseux. Par contraste, les eaux du type de Matlock (97% du flux thermique), possèdent des concentrations élevées en sulfates, provenant de l'interaction des eaux avec les évaporites enfouies, tandis qu'il n'existe aucune évidence chimique d'un écoulement sous les calcaires. Sur environ 5% de la surface des calcaires, les eaux souterraines alimentent des sources non-thermales. La dissolution du Gypse a produit une porosité tertiaire significative et une perméabilité dans les aquifères calcaires, et ceci est un précurseur essentiel au développement du drainage karstique.

Resumen Las aguas termales potencialmente proporcionan información sobre procesos geoquímicos que actúan a profundidad en acuíferos. Nuevos datos isotópicos de sulfatos, carbón inorgánico y estroncio en aguas termales y no-termales de un acuífero importante de caliza en Derbyshire, Inglaterra se utilizan para delinear las fuentes de sulfato y la evolución de aguas subterráneas.

Las aguas subterráneas no muy profundas adquieren sulfato a través de la oxidación de minerales de sulfuro y poseen carbón inorgánico disuelto (DIC) relativamente deplatado de ^{13}C. Las aguas termales muestran un ratio Sr/Ca relativamente alto y poseen (DIC) más enriquecido en ^{13}C, como resultado de la mayor interacción de roca-agua. En otros aspectos, los aguas termales definen dos grupos distintivos. Las aguas termales que ascienden en Buxton tienen mas Mg, Mn y $^{87}Sr/^{86}Sr$ y menos Ca and SO_4, indicando flujo de acuíferos de areniscas profundas por un sendero de alta permeabilidad en la caliza.

Received: 24 December 2005 / Accepted: 27 December 2005
Published online: 13 April 2006

J. Gunn · D. J. Lowe
Limestone Research Group, University of Huddersfield, Queensgate, Huddersfield, HD1 3DH, UK

S. H. Bottrell (✉)
Earth Sciences, School of Earth and Environment, University of Leeds,
Leeds, LS2 9JT, UK
e-mail: simon@earth.leeds.ac.uk

S. R. H. Worthington
Worthington Groundwater,
55 Mayfair Avenue, Dundas, Ontario, Canada, L9H 3K9

 DOI 10.1007/s10040-006-0022-7

En contraste el tipo de agua - Matlock (97% del flujo termal) posee altas concentraciones de sulfato, derivado por interacción con evaporitas enterradas, sin evidencia química de flujo debajo de la caliza. Aproximadamente 5% del agua del área de la caliza se fluye al grupo de manantiales de Matlock a través de un flujo regional profundo y el resto fluye por senderos locales poco profundos a muchos de los manantiales no-termales. La disolución de yeso ha producido porosidad terciaria importante así como permeabilidad en el acuífero de carbonato y este es un precursor esencial del desarrollo de drenaje kárstico.

Keywords England · Hydrochemistry · Karst · Stable isotopes · Thermal conditions

Introduction

In most limestone aquifers the original primary (matrix) permeability is low but there is a higher secondary (fracture) permeability. This is enhanced by the effects of carbonate dissolution to give an even higher tertiary (channel) permeability (Worthington and Smart, 2004). Numerical modelling has shown that conduit systems commonly develop over periods of tens of thousands of years in the vadose zone and the upper part of the saturated zone in a wide range of hydrological situations (Dreybrodt 1996; Hanna and Rajaram 1998; Gabrovšek and Dreybrodt 2001). These models represent local flow systems in the terminology of Tóth (1963). Processes acting deep within limestone aquifers are not readily amenable to study, yet may profoundly affect the subsequent, shallower permeability enhancement of the aquifer. Usually, chemical evidence of processes operating deep within an aquifer is masked by dilution or attenuation in shallower groundwaters, which tend to have shorter residence times and far higher flow rates than deep waters. Deep boreholes and tunnels can give insights into processes affecting deep groundwaters, but are rare. Occasionally, deep waters flow to the surface at springs in a relatively unmodified form and can be distin-

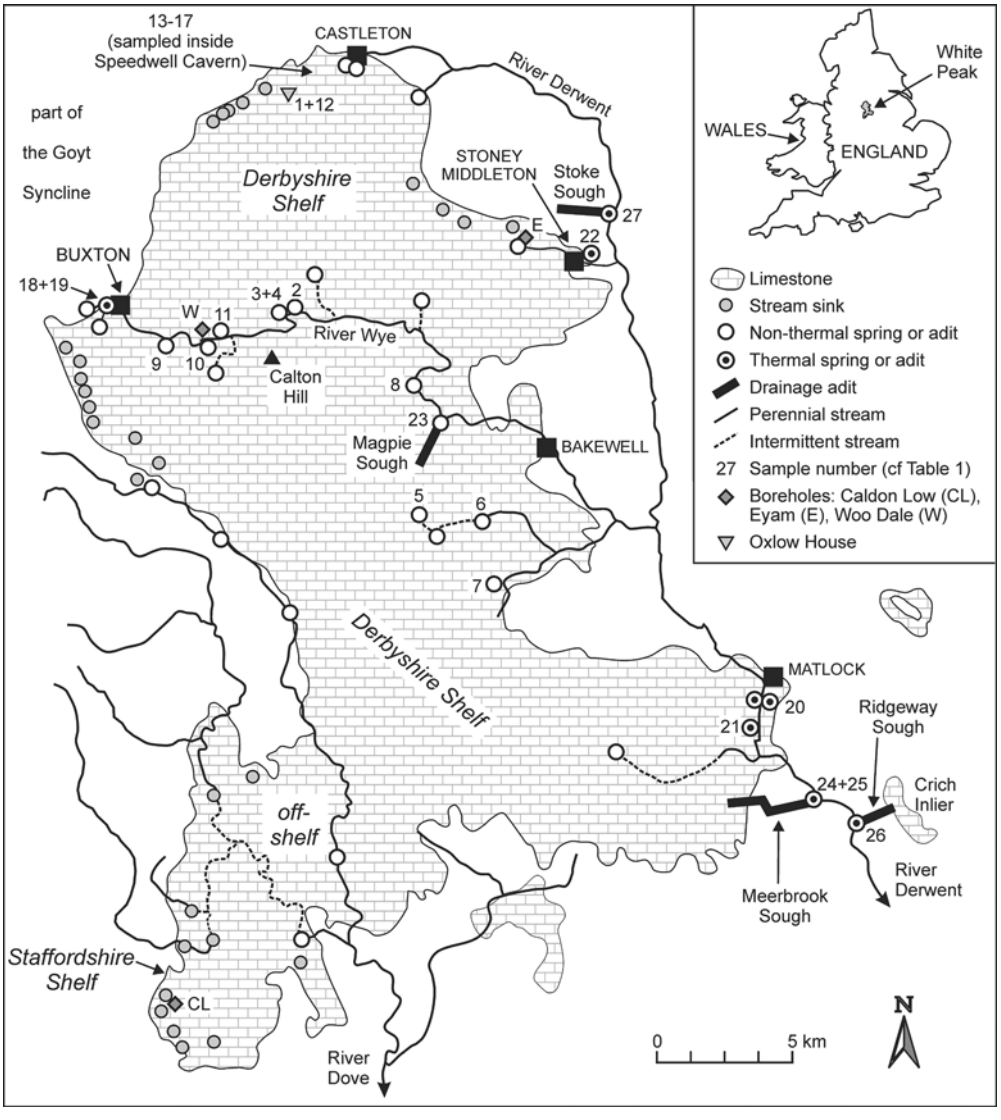

Fig. 1 Geological map of the White Peak with locations of sites mentioned in the text

 DOI 10.1007/s10040-006-0022-7

guished from shallow groundwaters by associated thermal and chemical anomalies. Such waters provide a natural window through which the deeper parts of the aquifer may be viewed. In the vast majority of cases, though, the geochemical and other characteristics of accessible groundwater are dominated by the shallow component. Consequently, most studies of secondary porosity and permeability development in limestone aquifers have focussed on shallow settings. This paper reports studies on thermal groundwater springs representing regional flow (Tóth 1963) that were undertaken to elucidate processes acting deep within a limestone aquifer.

Part of the Peak District in central England comprises a significant upland area dominated by carbonate lithologies, mainly limestone with minor dolomite, that is commonly known as the White Peak (Gunn et al. 1998)—shown in Fig. 1. The limestones form a regionally significant aquifer and groundwaters flow to a large number of springs, some of which are thermal. The thermal springs have stable and distinctive chemistry and low tritium concentrations (e.g. Edmunds 1971; Christopher and Wilcock 1981; Pentecost 1999), all factors indicating a component of flow via deep pathways. In this study the chemical and thermal characteristics of these waters, together with new sulphate, dissolved inorganic carbon (DIC) and strontium isotope data, are used to infer processes acting deep within the limestone aquifer. This evidence is used to constrain the depth to which these waters have penetrated, the amounts of water transmitted via deep flowpaths, the origins of the distinctive thermal water chemistry and the implications for porosity and permeability development at depth. A hydrogeological model for the aquifer system is derived and the implications for deep porosity/permeability development in the regional aquifer are examined.

Geological setting

Springs sampled during this study issue naturally or via mine drainage adits (locally called soughs) from various beds within a carbonate-dominated Dinantian (Carboniferous) sequence. Formational terminology recommended for the carbonate units by Aitkenhead and Chisholm (1982) remains in use, and the entire carbonate succession is now included within the Peak Limestone Group (Waters et al. in press).

In this area the Peak Limestone Group comprises thickly bedded, generally pale grey shelf limestones, about 2000 m in total thickness. The uppermost 600 m are exposed, and are relatively uniform across the northern and eastern White Peak and in the southwest whereas variable dark grey offshelf limestones, shales and sandstones occur between the Derbyshire and Staffordshire shelf areas (Fig. 1). Particularly in the north and west discontinuous fringing reef limestones border the shelf; elsewhere reef knolls grew locally in shallow lagoons.

Beneath the Derbyshire shelf, early Dinantian rocks were proved in the Woo Dale (Cope 1973, 1979) and Eyam (Dunham 1973) boreholes, where thick dolomitic and evaporitic beds overlie Lower Palaeozoic sedimentary and volcanic rocks. Dolomitic beds within the Woo Dale Limestone reach surface locally, but older evaporites do not crop out. Beneath the Staffordshire shelf, the Caldon Low Borehole (Institute of Geological Sciences 1978) proved early Dinantian dolomitic limestones and sandstones overlying Devonian arenaceous rocks.

Discontinuous local chert beds, argillaceous or coaly layers, dolostone, and zones of silicification and secondary dolomitisation interrupt the limestone sequence. Lavas, tuffs and mafic igneous intrusions occur in the north and east, with more widespread thin clay partings, of volcanic origin, termed ‘wayboards’. Some wayboards, lavas and tuffs overlie paleokarstic surfaces, and it is recognised that these beds have influenced the establishment and guidance of underground drainage routes within the otherwise relatively uniform carbonate mass.

The Peak Limestone Group forms one major and several smaller inliers (Fig. 1) surrounded by younger Carboniferous beds, and is overstepped in the south by Triassic rocks. Preserved patches of younger rock overlying the limestones include outliers of Namurian clastic rocks (also seen as neptunean fill in paleokarstic cavities) and ‘pocket deposits’, the remnants of a formerly extensive Neogene cover.

West of the White Peak, Silesian clastic rocks underlain by Dinantian carbonate rocks not unlike those described above form a series of major, more or less N–S trending, synclines and anticlines. Immediately west of the Peak, the Goyt Syncline (Fig. 1) extends more than 30 km from around Leek (20 km southsouthwest of Buxton) almost as far as Glossop (20 km north of Buxton), where it ceases to be recognizable. The fold, which plunges both northwards and southwards towards Chapel-en-le-Frith (8 km north of Buxton) is clearly expressed in the landscape, with its flanks marked by crags of Namurian sandstone. In the core of the syncline small outliers of Westphalian strata are preserved above the Namurian sequence, which in turn overlies Dinantian carbonates at depth. About 25 km west of the westernmost carbonate outcrops of the White Peak, carbonates are exposed along the Astbury Anticline, close to Congleton and ~20 km west of Buxton (Fig. 1). As buried carbonates also lie relatively close to the present surface within other anticlines between Congleton and the Peak, the original continuity of Dinantian rocks at depth between the Peak and the provings to the west is relatively certain.

In this paper the term ‘Peak District Dome’ is used in preference to the more commonly used ‘Derbyshire Dome’ as the Peak District also includes part of Staffordshire. However, it is recognised that the term is somewhat misleading, as it masks significant structural complexity. Uplift of the massif was already taking place during Dinantian times. Present geometry reflects interference of folds on three major trends (approximating to W–E, N–S and NW–SE), imposing a complex pattern of asymmetrical troughs, domes and monoclinal flexures. Innumerable minor interference ripples cross the limbs of the regional folds, and the local attitude of confined and unconfined hydraulically favourable

 DOI 10.1007/s10040-006-0022-7

beds has significant effect on underground drainage, even where dips and fold plunges are gentle.

Faults of all scales affect the Dinantian rocks, and movement began locally during late Dinantian times. Common trends are WNW–ESE, WSW–ENE and approximately N–S, but these are generalisations and many faults display arcuate traces. Many faults have been reactivated, some with a different sense of displacement, and strike-slip movement is evident locally. Commonly faults are assumed to provide fracture permeability within otherwise low permeability sequences, but they may also truncate or divert underground drainage routes within stratigraphically-guided zones of conduit permeability. Many faults or fault-related joint fractures in the White Peak are mineralised. Veins and related unmineralised cavities influenced underground drainage, and human activity, in mining the veins and in cutting deep drainage adits, has caused significant modification of underground flow patterns.

According to Smith et al. (1985) the northern White Peak is underlain by two southwestward-dipping basement tilt blocks, separated by the Bakewell Fault, a major growth fault that dips towards the north. There is little surface expression of these deep structures, but the tilt-block/growth fault model provides one plausible explanation for significant thickness and depth variations in the Dinantian sequence and for the known distribution of early Dinantian evaporitic rocks.

Previous work on limestone groundwaters

Carbonate rocks are highly soluble due to the presence of dissolved CO_2 (carbonic acid) in recharge waters as a result of soil zone respiration. Hence, spring waters rising from the limestone should have solute chemistry dominated by dissolution reactions in the carbonate system, i.e. Ca-Mg-(Sr)-HCO_3^- compositions. However, regional studies of spring water chemistry in the White Peak (Christopher et al. 1977; Edmunds 1971) have shown that sulphate is present in significant concentrations in many spring waters, especially thermal waters in the Matlock area. Various hypotheses have been advanced for the origin of elevated sulphate concentrations in limestone groundwaters, both in general and in the White Peak in particular, and these are reviewed below.

Christopher et al. (1977) attributed elevated sulphate in White Peak springs to weathering of galena and sphalerite in ore bodies, a source confirmed as significant by isotopic studies of sulphate sources in the Castleton catchment (in the north of the White Peak) (Bottrell et al. 2000). At Castleton, other significant sulphate sources identified by Bottrell et al. (2000) were shale weathering and agricultural practices on non-limestone catchments (which supply water to the limestone aquifer via sinking streams) and oxidation of pyrite in the limestone. Similarly, Moncaster et al. (1992, 2000) demonstrated that anthropogenic sulphur sources (atmospheric pollutants and agrichemicals) and oxidation of pyrite in the aquifer matrix dominated the sulphate budget of the Lincolnshire Limestone aquifer (eastern England). Further afield, both Crabtree and Trudgill (1984) and Langmuir (1971) inferred dominantly anthropogenic sources for sulphate (atmospheric pollution and agrichemicals, respectively) in groundwaters of the Magnesian Limestone of eastern England and limestones of central Pennsylvania, USA, respectively.

Edmunds (1971) noted a general East–West trend in both sulphate and strontium concentrations in the White Peak groundwaters and correlated this with the distribution of mineralisation, suggesting that dissolution of impure (Sr-rich) barite in mineralised areas contributed these components. Worthington and Ford (1995) envisaged a rather different scenario. They attributed high sulphate in the thermal springs at Matlock to dissolution of gypsum or anhydrite evaporite deposits at depth in the carbonate sequence, by a component of deep groundwater (under)flow. This deep component then flowed to springs at the lowest elevation limestone outcrop in the Derwent valley. Their model is similar to that proposed by Krothe and Libra (1983), who used sulphur isotopic compositions to identify a significant gypsum sulphate component associated with flow to karst springs in southern Indiana, USA.

The only study of deep groundwater diagenesis in the same Carboniferous Limestone aquifer was undertaken by Downing (1967) who used analyses of Carboniferous Limestone formation waters from oil exploration and production wells 80 km east of Matlock (Fig. 1), where the aquifer is confined at depth. He noted a general increase in chloride and sulphate in the deeper waters. He considered evaporites as a possible source, but discounted them as the extent of evaporite deposits in the Lower Carboniferous was then thought more restricted than now known. He thus preferred oxidation of pyrite (or ore sulphide minerals in possible mineralised zones) as the sulphate source. However, he noted that the waters were effectively ‘stagnant’ and that dissolution or leaching of only relatively small amounts of these components was required. The resurging thermal waters, on the other hand, have a constant flow with essentially unchanging chemistry over the period they have been studied (see Pentecost, 1999) and thus require continuous replenishment of these salts.

Sampling and analytical details

Sampling rationale

Sampling sites were selected as far as possible to yield data representative of four types of ground and thermal waters present in the White Peak, viz:

1. Autogenic karst springwaters, i.e. those fed by catchments without sinking streams inflowing from non-karst catchments. These were sampled at natural surface springs, at percolation water inflows to caves and at one private supply borehole.
2. Thermal springs and wells, which divide geographically. There is a single thermal rising at Buxton and a number

 DOI 10.1007/s10040-006-0022-7

of thermal risings along the eastern side of the limestone outcrop from Stoney Middleton to Matlock (see Fig. 1). The latter group are referred to as the 'eastern group' or 'Matlock-type' waters in this work.

3. Mine drainage adits with no evidence of a thermal nature, i.e. with temperatures in the same range as non-thermal springs.
4. Mine drainage adits issuing thermal waters, i.e. at an average temperature above that of the non-thermal springs.

In addition, rain water was collected at a weather station at Oxlow House Farm near Castleton at the north of the White Peak (Fig. 1). In this work an annual average datum is used (April 1995–March 1996), calculated as the volume-weighted mean concentration and the mass-weighted mean sulphate isotopic composition.

Sampling and analytical procedures

Samples were collected from springs, wells, a supply borehole, drainage adits and underground locations. On site pH, temperature and conductivity of the waters were measured with portable meters, and titratable alkalinity was determined with a Hach digital titrator. Two aliquots were syringe filtered through 0.45 μm membranes in the field; one was kept unacidified and refrigerated for analysis for anion concentrations with a Dionex DX-100 ion chromatograph; the other was acidified with 2% 'Analar' nitric acid for cation analysis using an ARL Maxim ICP-AES system. Samples for Sr isotopic analysis were also filtered at collection but taken in specially-cleaned bottles and acidified with quartz-distilled HCl. In some cases a further sample was collected for total dissolved inorganic carbon (TDIC) isotopic analysis; an aqueous solution of $SrCl_2 + NH_4OH$ was used to precipitate $SrCO_3$ from the sample water and this was recovered by vacuum filtration (Bishop 1990). The $SrCO_3$ was reacted with phosphoric acid under vacuum to produce CO_2 for isotopic analysis (McCrea 1950). A fourth, larger sample was collected for sulphate isotopic analysis and filtered in the laboratory. This was adjusted to pH = 3.0 with HCl and heated to ~70°C before precipitation of sulphate as $BaSO_4$ by the addition of $BaCl_2$ solution. The precipitate was recovered on a 0.45 μm membrane filter, washed and dried. One aliquot was fluxed with $Na_3(PO_3)_3$ to produce SO_3, which was immediately reduced to SO_2 on Cu wool (Halas et al. 1982). Another aliquot was reacted with graphite to produce a $CO_2 + CO$ mixture; the CO was disproportionated to CO_2 with quantitative recovery of oxygen (McCarthy et al. 1997). All gases were purified using standard vacuum-cryogenic techniques and analysed for $^{34}S/^{32}S$ (SO_2), $^{13}C/^{12}C$ and $^{18}O/^{16}O$ (CO_2) on a VG SIRA 10 gas source isotope ratio mass spectrometer. Data are reported in standard δ notation in per mil (‰) enrichment or depletion of the heavy isotope relative to the V-CDT (sulphur), V-PDB (carbon) and V-SMOW (oxygen) standards (these are IAEA Vienna-defined standards, see Gonfiantini, 1978, 1984). Sr was separated from groundwater by standard ion exchange techniques and $^{87}Sr/^{86}Sr$ determined on a VG Isomass 54E mass spectrometer, courtesy of Dr. R. A. Cliff.

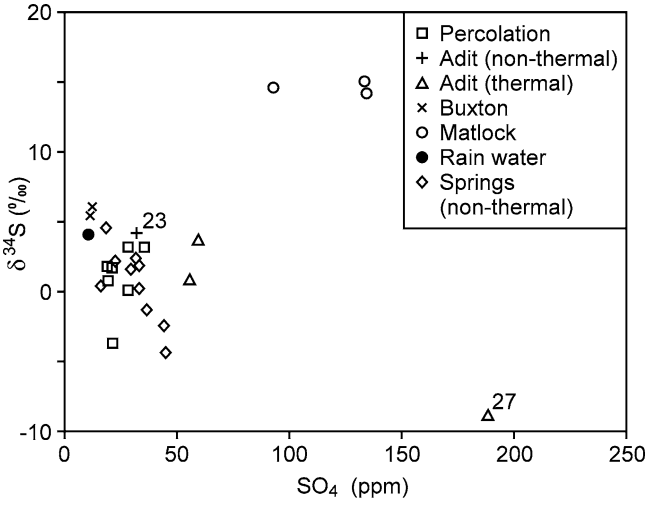

Fig. 2 Sulphate $\delta^{34}S$ plotted vs. sulphate concentration for all the analysed waters. Note the distinctive high concentration and $\delta^{34}S$ values of the Matlock-type thermal waters

Results and discussion

The cation, anion and light stable isotope analyses are presented in Table 1. Sulphate concentration is plotted against $\delta^{34}S$ of sulphate in Fig. 2 and this plot serves to distinguish the main water types.

Rainfall, spring and cave drip (percolation) waters

Spring and cave drip waters are Ca-HCO_3 waters and the $\delta^{13}C$ of the DIC (around −14‰, Table 1) shows the bicarbonate to be derived in roughly equal proportions from soil gas CO_2 and limestone carbonate (e.g. Bishop and Lloyd

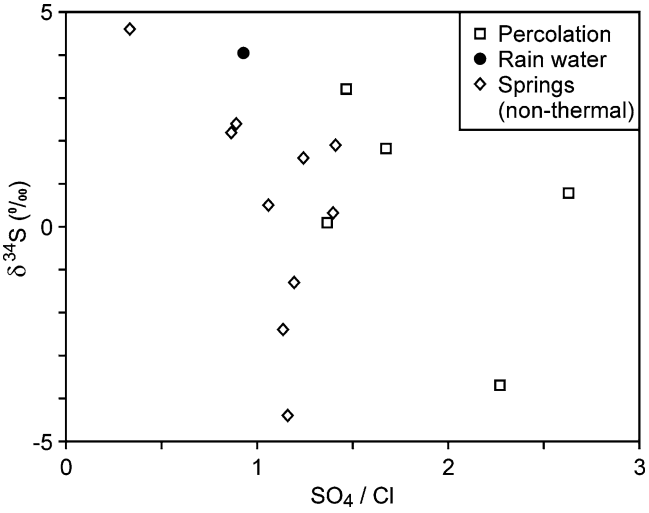

Fig. 3 Sulphate $\delta^{34}S$ plotted vs. SO_4^{2-}/Cl^- for average rainfall, non-thermal spring and cave drip waters

DOI 10.1007/s10040-006-0022-7

Table 1 Sample locations, types, chemical and isotopic analyses of all waters

Sample no	Sample location	Sample type	*T* (°C)	pH	Cond. (μS/cm)	HCO_3 (ppm)	Ca (ppm)	Mg (ppm)	Na (ppm)	K (ppm)	Sr (ppm)	SO_4 (ppm)	Cl (ppm)	NO_3 (ppm)	$\delta^{34}S$ (‰)	$\delta^{18}O$ (‰)	$\delta^{13}C$ (‰)
1	Oxlow House	Rain water	N/A	N/A	N/A	N/A	N/A	N/A	N/A	N/A	N/A	11.1	11.9	N/A	4.05	N/A	N/A
2	Cheedale Rising	Non-thermal spring	9.2	7.14	601	256	110.9	7.5	12.4	1.4		33.7	24.1	11.9	0.3	N/A	−14.7
3	Wormhill east	Non-thermal spring	8.7	7.39	598	217	90.3	7.1	20.4	4.1	0.11	44.6	39.3	10.6	−2.4	N/A	−14.7
4	Wormhill west	Non-thermal spring	9.8	7.37	595	215	89.9	7.1	19.4	4.1	0.11	45.5	39.2	12.1	−4.4	4.1	−16.3
5	Lathkill Dale	Non-thermal spring	8.8	7.25	579	233	107.7	2.2	11.4	2.2	0.16	23.0	26.5	15.1	2.2	3.9	−17.8
6	Lathkill Dale	Non-thermal spring	9.1	8.16	655	222	109.5	4.7	24.2	0.81	0.15	18.9	57.5	13.2	4.6	N/A	−16.5
7	Bradford Dale	Non-thermal spring	9.4	7.40	569	270	79.4	16.5	4.8	0.31	0.09	16.7	15.8	18.3	0.5	5.3	N/A
8	Lees Bottom	Non-thermal spring	11.5	7.89	631	239	103.8	6.1	13.1	1.2	0.20	37.2	31.2	17.7	−1.3	3.6	−14.0
9	Cowdale Spring	Non-thermal spring	8.8	7.53	596	198	120.8	6.5	10.2	0.4	0.4	30.2	24.3	14.6	1.6	5.7	−14.4
10	Ashwood Dale	Non-thermal spring	8.1	7.18	674	217	139.1	4.8	14.3	0.6	0.7	32.0	36.0	28.9	2.4	5.0	−15.6
11	Woo Dale Spring	Non-thermal spring	7.9	7.26	679	240	60.3	10.7	14.8	1.0	0.6	33.6	23.8	32.9	1.9	4.9	−16
12	Oxlow House	Percolation	12.6	7.34	539	241	116.4	1.2	8.0	1.5	0.07	29	21.2	10.9	0.1	N/A	N/A
13	Speedwell Cavern (CP)	Percolation	N/A	N/A	N/A	N/A	N/A	N/A	N/A	N/A	N/A	22.0	N/A	N/A	1.7	N/A	N/A
14	Speedwell Cavern (CP)	Percolation	N/A	N/A	N/A	N/A	92.3	1.7	4.5	1.0	0.12	20.0	7.6	8.6	0.8	N/A	N/A
15	Speedwell Cavern (CP)	Percolation	N/A	N/A	N/A	N/A	96.5	1.3	4.1	0.8	0.11	22.1	9.7	10.2	−3.7	N/A	N/A
16	Speedwell Cavern (CP)	Percolation	N/A	N/A	N/A	N/A	N/A	N/A	N/A	N/A	N/A	19.6	11.7	17.4	1.8	N/A	N/A
17	Speedwell Cavern (BP)	Percolation	N/A	N/A	N/A	N/A	98.7	2.3	12.1	14.0	0.14	28.5	19.4	30.8	3.2	N/A	N/A
18	St. Annes Well	Buxton-type spring	27.2	7.06	509	241	59.0	20.2	24.2	1.1		12.2	38.8	<0.05	5.5	10.5	−8.3
19	Pump Room	Buxton-type spring	N/A	7.40	N/A	248	61.6	21.2	24.9	1.0		12.8	34.9	<0.05	6.1	9.9	N/A
20	Matlock East Bank Rising	Matlock-type spring	20.5	7.11	819	246	94.6	26.6	22.9	1.1	1.71	133.9	47.8	3.1	15.0	15.1	−9.9
21	Matlock New Bath Hotel	Matlock-type spring	21.0	6.48	850	238	85.3	24.6	21.3	0.65	0.71	134.7	49.3	2.8	14.2	N/A	−12
22	Stoney Middleton thermal	Matlock-type spring	18.2	7.56	909	242	91.8	28.2	60.0	1.4	0.71	93.5	90.2	1.6	14.6	14.0	−8.1
23	Magpie Sough	Non-thermal adit	9.4	7.80	568	220	90.1	9.1	7.7	0.78	0.45	32.6	47.2	11.7	4.2	7.5	−13.5
24	Meerbrook Sough	Thermal adit	17.0	7.98	608	212	85.9	22.1	12.8	1.1	0.50	59.8	24.7	10.2	3.7	8.7	−12.6
25	Meerbrook Sough	Thermal adit	17.0	7.89	612	246	82.3	20.9	11.9	0.90	0.48	59.5	25.3	10.1	6.3	N/A	N/A
26	Ridgeway Sough	Thermal adit	14.4	6.75	373	229	83.4	6.3	11.1	4.4	0.11	55.9	23.7	17.3	0.8	4.0	−14.9
27	Stoke Sough	Thermal adit	14.2	6.54	1052	193	111.5	25.1	45.0	3.4	1.41	188.3	77.0	2.5	−8.8	3.8	−9.0

Percolation: autogenic percolation water from the limestone aquifer. Speedwell Cavern (CP) and Speedwell Cavern (BP) refer to two locations in Speedwell Cavern, Cliff Passage and Boulder Piles, respectively. ($\delta^{18}O$ and $\delta^{34}S$ were measured on sulphate and $\delta^{13}C$ on TDIC).

DOI 10.1007/s10040-006-0022-7

1990). The annual average rainfall contains 11.1 ppm sulphate with $\delta^{34}S$ of +4.1‰. This point lies to one end of the distribution of the karst spring waters, which range up to 46 ppm sulphate with more depleted isotopic compositions (down to $\delta^{34}S = -4.4$‰). Clearly, the trend to more ^{34}S-depleted concentrations with increased sulphate concentrations is likely to result from addition of varying amounts of ^{34}S-depleted sulphate during transit of groundwater. The plot of $\delta^{34}S$ vs. SO_4/Cl for karst spring and percolation waters in Fig. 3 confirms that this is the case, as differential evaporative concentration of sulphate in the soil zone prior to recharge (which might also produce a range of SO_4 concentrations) would not affect SO_4/Cl ratios. The data exhibit a spread away from the rainfall composition toward more ^{34}S-depleted compositions with increasing SO_4/Cl, but do not follow a single trend, indicating that sulphate is added from more than one source with different, but always ^{34}S-depleted, isotopic composition. The isotopic composition of the sulphate added is consistent with the range of isotopic compositions of both mineral-vein sulphides hosted by the limestone (−23 to +7‰, Robinson and Ineson 1979; Ewebank et al. 1995) and diagenetic sulphide in the limestone (−22.3 to +3.4‰, Bottrell et al. 2000). The $\delta^{18}O$ of sulphate in these waters is consistent with addition of sulphate produced by oxidation of sulphide in an oxygenated environment (e.g. Van Stempvoort and Krouse 1994).

The cave drip waters have low Mg concentrations and low Mg/Ca ratios, as a result of being derived from low Mg-limestone in this catchment. Spring waters have a higher range of Mg concentrations and Mg/Ca ratios (Table 1, Fig. 4) as a result of interaction between groundwater and dolomitic limestones; the range of values is a function of both the variable presence of dolomite in the aquifer matrix and residence time. Thus, apart from the usual carbonate system reactions, the chemical evolution

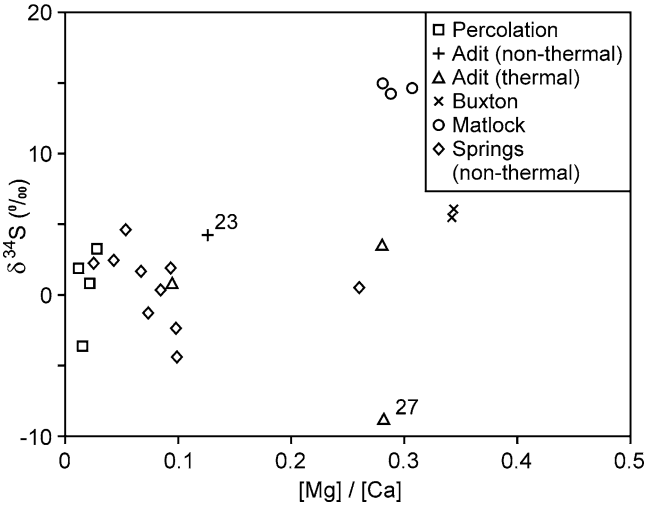

Fig. 4 Sulphate $\delta^{34}S$ plotted vs. Mg/Ca for all analyzed waters. Note the high Mg/Ca of all the thermal waters (Matlock-type, Buxton and thermal adits) compared to the non-thermal spring and cave drip waters

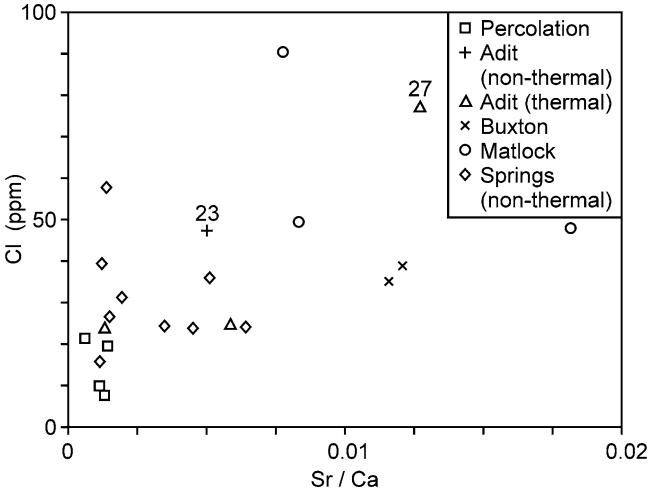

Fig. 5 Chloride concentration plotted vs. Sr/Ca for all analyzed waters. Note the elevated Sr/Ca of all the thermal waters (Matlock-type, Buxton and thermal adits) compared to the non-thermal spring and cave drip waters and high chloride concentration of the Matlock-type thermal and thermal adit waters

of spring waters and cave drip waters is significantly affected by addition of sulphate from oxidation of sulphide minerals.

Thermal springs

The thermal spring waters of the White Peak have long attracted scientific interest and, as a result, there is a considerable historical database of chemical analyses. The present analyses (Table 1) are similar to previous ones and confirm the observation of Pentecost (1999) that there has been no significant change in their chemistry during the history of their study. The geographical division of the thermal spring waters is reflected in a strong differentiation in their chemistry: the Buxton waters are relatively dilute and distinguished by their low Ca and high Mg/Ca, whereas the eastern (Matlock-type) group have much higher sulphate concentrations (Table 1, Fig. 2). Both groups of thermal springs are distinguished from the spring and percolation waters by relatively elevated Sr/Ca ratios and generally higher Cl concentration (Fig. 5). The higher Sr/Ca presumably results from increased interaction between these waters and the limestone aquifer material. Extensive carbonate dissolution/reprecipitation reactions concentrate Sr, as an incompatible element, in the aqueous phase, whereas Ca concentration remains constant at calcite saturation. The ^{13}C content of TDIC confirms this, as both groups of thermal waters have TDIC enriched in ^{13}C (−8 to −10‰$_{PDB}$) compared to the spring waters (around −14‰$_{PDB}$; see Fig. 6). Such enrichments of ^{13}C in TDIC are also the result of extensive dissolution/reprecipitation of carbonate minerals (e.g. Bishop and Lloyd 1990). The long residence times of these thermal waters required for such extensive groundwater-aquifer interaction are confirmed by the low tritium concentrations measured in some of these waters by Edmunds (1971).

DOI 10.1007/s10040-006-0022-7

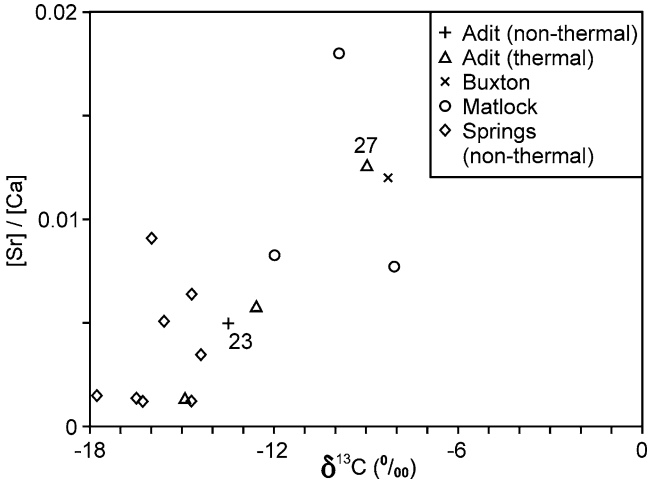

Fig. 6 Sr/Ca plotted vs. $\delta^{13}C$ of TDIC for all analyzed waters. Non-thermal spring waters are ^{13}C depleted and have low Sr/Ca compared to the thermal springs and adits. Enrichment of ^{13}C in DIC and increased Sr/Ca can both result from extensive carbonate dissolution and reprecipitation

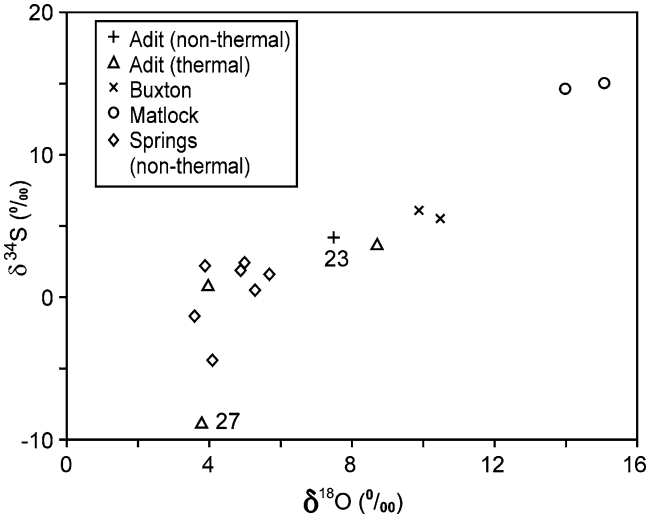

Fig. 7 Sulphate $\delta^{34}S$ plotted vs. sulphate $\delta^{18}O$ for all analyzed samples. Note the clear distinction between the different sample groupings

The isotopic composition of sulphate also differs between the two groups of thermal water (Figs. 2 and 7). The Buxton waters have $\delta^{34}S \sim +6‰$ and $\delta^{18}O \sim +10‰$, whereas the eastern group has $\delta^{34}S \sim +15‰$ and $\delta^{18}O \sim +14‰$. These latter values correspond exactly with isotopic compositions of marine sulphate from Lower Carboniferous evaporites in Britain (Claypool et al. 1980; Taylor 1983; Crowley et al. 1997). Such evaporites are known from the eastern side of the White Peak in a borehole core from Eyam, so dissolution of evaporites would appear to be the source of high sulphate and chloride concentrations in the eastern group thermal waters. These ^{34}S-enriched compositions are also within the wide range of compositions (5–23‰) reported for barite sulphate associated with mineralisation (Robinson and Ineson 1979). However, evaporite dissolution (rather than barite dissolution as suggested by Edmunds 1971) is considered to be the likely source of this sulphate because of (i) the exact match of both $\delta^{34}S$ and $\delta^{18}O$ in dissolved sulphate with that of Lower Carboniferous evaporite sulphate; (ii) the very low solubility of barite; and (iii) the association of sulphate with chloride. The chloride can readily be provided by dissolution of chloride evaporite minerals associated with anhydrite or gypsum, but it is not a component of mineralised vein assemblages.

The Buxton thermal waters have far lower sulphate concentrations than the eastern group of thermal springs, but their high Sr/Ca ratio and ^{13}C-enriched TDIC attest to their long residence time. Some aspects of their chemistry and isotopic compositions suggest that they could be mixtures of the Matlock-type thermal waters and shallow spring/percolation waters (e.g. Figs. 4, 5 and 7). However, because of their high Mg/Ca (Fig. 4) and very low sulphate concentration (Fig. 2), the Buxton waters cannot be diluted Matlock-type thermal waters, even if the diluent were unaltered modern rainwater. The high Mg/Ca in the Buxton waters is also unlikely to originate from leaching of Mg from lavas or 'wayboards' since such waters are characterised by high sulphate (Christopher and Wilcock 1981). The low sulphate concentration of the Buxton waters cannot be the result of removal of sulphate from a Matlock-type water by bacterial sulphate reduction (followed by some dilution). This would produce a residual sulphate that was very strongly enriched in ^{34}S and ^{18}O (i.e. at more positive values on Fig. 7 than the Matlock-type waters, rather than the less positive values that they actually have). Such isotopic enrichments are a consequence of the large isotopic fractionations associated with bacterial sulphate reduction and the large proportion of sulphate that would have to be removed from a Matlock-type water (Chambers and Trudinger 1979; Strebel et al. 1990).

In pre-industrial times, rainwater would have had lower sulphate concentration, due to the absence of sulphate derived from fossil fuel burning. Such an unpolluted rainwater would, however, be dominated by marine-derived sulphate aerosol and would thus have a far more ^{34}S-enriched isotopic composition (see e.g. McArdle and Liss 1996; Bottrell and Novak 1997). Edmunds et al. (1995) estimate a value of $+7‰$ from isotopic studies of sulphate in the Triassic aquifer south of the Peak District but, Coulson et al. (2005) find evidence for pre-anthropogenic atmospheric sulphur inputs closer to $+20‰$ in the northern Peak District, suggesting that the estimate by Edmunds et al. may be influenced by soil zone or other sulphur sources. The Buxton thermal water sulphur isotopic composition lies on an extension of the spring and percolation water trend in Fig. 2 and this suggests that it represents a mixture of pre-industrial recharge (with $\delta^{34}S > +10‰$) with some sulphate derived from sulphide oxidation. The $\delta^{18}O_{sulphate}$ of these waters, at around $+10‰$, is considerably enriched in ^{18}O relative to the spring/percolation water sulphate, probably the result of the ^{18}O-enriched composition of the marine-derived sulphate (at $\sim+12‰$), which dominated the pre-industrial recharge. Such an origin is consistent

DOI 10.1007/s10040-006-0022-7

with the relatively high Cl concentrations (~40 ppm, Fig. 5) and low SO_4/Cl (Table 1) in the Buxton waters. The marine aerosol-dominated rainwater recharge would have had lower SO_4/Cl than modern rainwater and the Cl concentration of the Buxton waters is no higher than the highest non-thermal springwaters (Fig. 5).

Non-thermal adit drainage

One mine-drainage adit was sampled that had no evidence of increased water temperature (Magpie Sough, sample 23). On Figs. 2, 4 and 5 this sample lies displaced from the bulk of the spring water data, toward the compositions of the Matlock-type thermal waters. This suggests that a small component of Matlock-type thermal water is mixing with shallow spring/percolation water at this site without causing any measurable thermal perturbation. This hypothesis seems reasonable, given the geographical location of Magpie Sough relative to the distribution of the eastern group of thermal waters (see Fig. 1). Edmunds (1971) also noted elevated Sr concentrations in non-thermal mine drainage waters compared to springwaters, and attributed this to interaction between normal shallow groundwater and ore minerals containing high Sr concentrations (principally barite). However, the isotopic data does not support this and instead suggests water mixing, which is perhaps more reasonable given the very low solubility of barite. This mixing may have been induced by local lowering of groundwater head by mine drainage, resulting in an upward migration of deeper water with thermal-type chemistry.

Thermal adit drainage

A number of mine drainage adits on the east side of the White Peak have mean temperatures greater than those of normal springs. Three such waters were sampled and two (#24 and #26) show similar chemical and isotopic characteristics (Figs. 2, 4 and 5) to the Magpie Sough water (#23) discussed above, suggesting that they are similar mixtures of Matlock-type thermal waters and shallow groundwater. Again the geographical location of these sites (Fig. 1) is consistent with this hypothesis and lowering of groundwater heads by mine drainage may have promoted upward movement and resurgence at surface of thermal water. The third of these sites (#27) has very high concentrations of sulphate (Fig. 2) and chloride (Fig. 5), very ^{13}C-enriched TDIC (Fig. 6) and high Sr/Ca (Fig. 5). These features are all consistent with a large component of Matlock-type thermal water, as is its geographical location. However, this water differs from the others in having very ^{34}S-and ^{18}O-depleted sulphate isotopic compositions (Fig. 7) and has higher sulphate concentration and SO_4/Cl (Fig. 2, Table 1) than the Matlock-type thermal waters. This water then cannot be either a Matlock-type thermal water or a simple dilution with shallow groundwater. However, if a thermal water were mixed with an oxygenated shallow groundwater that had undergone extensive interaction with pyrite, then the observed chemical and isotopic compositions would result. Interaction between oxygenated water and pyrite in a carbonate aquifer is described by the overall reaction (Nicholson et al. 1988):

$$FeS_2 + 4CaCO_3 + 3.75O_2 + 3.5H_2O \Rightarrow 2SO_4^{2-} + 4HCO_3^- + 4Ca^{2+} + Fe(OH)_3 \quad (1)$$

where $Fe(OH)_3$ is a stable end product provided that a near-neutral pH is maintained by calcite dissolution. This reaction would add sulphate to the groundwater mixture, increasing SO_4 concentration and SO_4/Cl above that predicted for a simple mixture and this sulphate would be ^{34}S-depleted if it were derived from pyrite of diagenetic or mineral-vein origin (Robinson and Ineson 1979; Ewebank et al. 1995; Bottrell et al. 2000). The δ^{18}O of the sulphate formed in this way would also be much lower than the evaporitic values of Matlock-type thermal waters (e.g. Van Stempvoort and Krouse 1994), as we observe. The reaction also adds DIC derived from ^{13}C-rich calcite (both marine carbonate aquifer matrix and mineral vein calcite have δ^{13}C around 0‰$_{PDB}$, Robinson and Ineson 1979) to the groundwater, consistent with the measured DIC δ^{13}C of −9‰, the ^{13}C-rich calcite-derived DIC offsetting the effect of the ^{13}C-depleted shallow groundwater DIC in the mixture.

Strontium isotopic compositions

Both non-thermal and Matlock-type thermal springs have closely similar strontium isotopic compositions that are slightly enriched in radiogenic ^{87}Sr compared to limestones which will have Carboniferous marine compositions (Table 2). This small enrichment could result from interaction with K-bearing minerals in soils, in igneous rocks or more clay-rich lithologies. Importantly, the Sr isotopic data do not indicate any significant interaction between the Matlock group thermal waters and lithologies outside the Lower Carboniferous carbonate/evaporite sequence, the

Table 2 Strontium isotopic analyses of Peak District Dome groundwaters and best estimate of Lower Carboniferous seawater Sr isotopic composition

Sample location numbers are as Table 1. Precision and accuracy of all water analyses is ±0.00003.

Sample location	Date of sampling	Water type	^{87}Sr/^{86}Sr
2	29th January 1998	Non-thermal spring	0.70853
10	29th January 1998	Non-thermal spring	0.70864
18	29th January 1998	Buxton thermal water	0.71020
19	29th January 1998	Buxton thermal water	0.71022
21	29th January 1998	Matlock-type thermal water	0.70861
22	12th March 1998	Matlock-type thermal water	0.70884
Burke et al. (1982)	N/A	Lower Carboniferous sea-water	0.7081–0.7084

 DOI 10.1007/s10040-006-0022-7

rocks of which are dominated by a Lower Carboniferous sea-water Sr isotopic composition. The Buxton thermal water is distinctly ^{87}Sr-enriched compared to the other waters. This indicates that the Buxton thermal waters have interacted with a source of radiogenic Sr not seen in the other waters, and reinforces the distinction between the Buxton and Matlock-type thermal waters.

Thermal output of the springs

The thermal output of the thermal springs is given by the relationship:

$$\text{Thermal output (kW)} = 4.2 \times T_{\text{diff}} \times \text{discharge (ls}^{-1}\text{)}, \quad (2)$$

where T_{diff} is the temperature difference (in °C) between thermal and non-thermal springs. Edmunds (1971) gives discharge and temperature data for all the significant thermal risings. The calculated thermal output is plotted (on a logarithmic scale) against spring elevation in Fig. 8. The eastern group of thermal risings define a clear trend on this plot with increasing thermal output at lower elevation. Two of the thermal adit risings are displaced below/to the left of the main trend, possibly because these constructed features have not attained the same thermal equilibrium as the natural springs or, in the case of Ridgeway Sough, because the waters issue from the Crich Inlier, a different hydrogeological setting to the other thermal risings in the Derwent valley. The Buxton waters lie well away from the trend and have a higher temperature (27.5°C) than any of the other thermal risings (highest 19.8°C). A temperature difference of 18.5°C at surface for the Buxton water implies a thermal reservoir temperature (T) of ~48°C (Turcotte and Schubert 1982), or a depth around 1 to 1.5 km (Oxburgh et al. 1980; Downing and Gray 1986). On the same basis, the warmest of the eastern (Matlock) group thermals would have a thermal reservoir T of ~30°C, or a depth less than 1 km.

Barker et al. (2000) considered the effects of thermally-generated density differences on the flow of the thermal spring at Buxton and concluded that the flow of thermal water was principally driven by such a mechanism. Their model was supported by comparison with recent hydrograph and rainfall data. A similar mechanism could be partly responsible for the upflow of the eastern group of thermal waters, though their cooler temperatures would make any driving force less potent. However, the focusing of the thermal output of the eastern group thermal waters toward lower altitude risings indicates a significant component of their flow must relate to head differences between their recharge and discharge zones.

Porosity generation at depth

The Matlock-type thermal waters contain around 100 ppm of sulphate derived by gypsum dissolution at depth, corresponding to 140 ppm dissolved $CaSO_4$ (equivalent to 176 mg gypsum dissolved by each litre). Using the total thermal output from the Matlock group of thermal risings, and assuming a discharge temperature unmodified by shallow mixing with non-thermal water of 20°C, the total discharge of thermal water can be calculated as 480 l s^{-1}, or 15×10^6 m^3 year^{-1}. The rate of dissolution of gypsum is thus ~2300 tonnes year^{-1} or ~1100 m^3 gypsum removed per year. This is a significant rate of porosity generation, even when the areal extent of the aquifer system (maximum 540 km^2) is taken into account. It is impossible to know how localised or dispersed this gypsum dissolution is within the deep aquifer, but this rate equates to an increase in aperture of 1 mm per year over a 1000 km network of 1 m wide fractures.

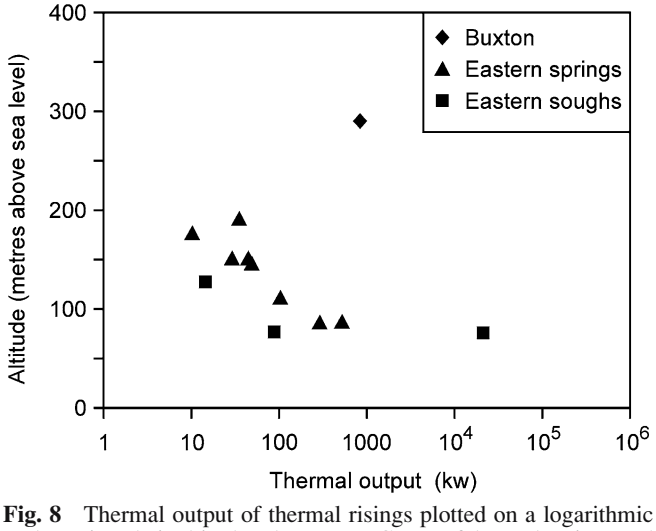

Fig. 8 Thermal output of thermal risings plotted on a logarithmic scale against their altitude. The Eastern Group of thermal springs and adits lie on a trend with increasing output at lower elevations. The Buxton thermal rising plots well away from this trend

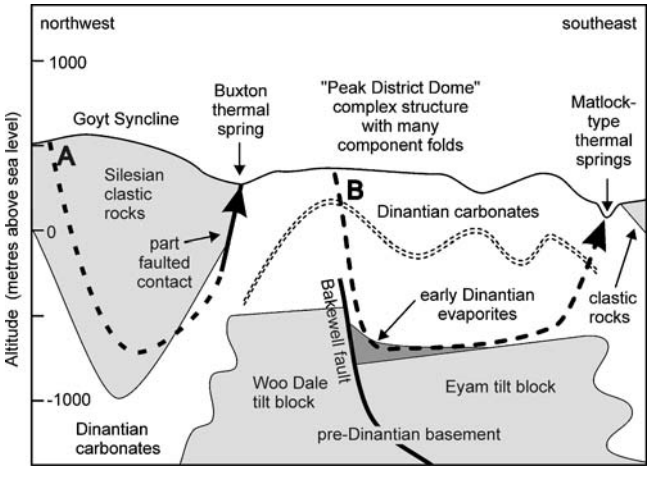

Fig. 9 Composite conceptual model of major geological components and deep thermal groundwater flow between the Goyt syncline in the west and the Derwent valley in the east. All topographical and geological relationships are greatly simplified. The nature and position of the Bakewell Fault and related basement blocks (Smith et al. 1985) are speculative. Vertical exaggeration about ×20

DOI 10.1007/s10040-006-0022-7

Hydrogeological model

A conceptual hydrogeological model for the thermal waters of the White Peak is illustrated in the form of a west–east cross section in Fig. 9. Dashed arrows indicate the flow paths of Buxton (A) and Matlock-type (B) thermal waters. The Buxton waters are shown as migrating to ~1500 m depth in the Goyt syncline before rising as a result of thermal effects, the flow possibly being focussed by faulting at the limestone contact. Matlock-type waters are shown as migrating to ~800 m depth to interact with evaporite deposits. Their return flow to surface may be driven by a combination of elevation head difference between the recharge area on the limestone plateau and the Derwent valley (hence the higher thermal fluxes at lower elevation thermal springs) and by thermal effects similar to, but less efficient than, those at Buxton. Upward return flow would be via cross-stratal leakage on fractures and focussed by plunging antiformal structures. The Matlock and Buxton groups of thermal waters are distinct in terms of their chemistry and isotopic compositions. These clear distinctions suggest very different origins for the two types of thermal waters. The Buxton waters are more dilute and appear to be pre-industrial recharge that has undergone limited interaction with sulphide minerals. The 1–1.5 km depth inferred for the thermal flow at Buxton is comparable to the thickness of Namurian (Millstone Grit) and Westphalian (Coal Measures) clastic sediments (~1400 m; Aitkenhead et al. 1985) overlying the limestone in the Goyt Syncline to the west of Buxton. The Buxton water has elevated ^{87}Sr, probably due to interaction with clay-rich detrital rocks, and high Mn (75 $\mu g\,l^{-1}$ vs. ~1 $\mu g\,l^{-1}$ for the eastern group thermal waters; Edmunds 1971), also indicative of interaction with detrital sedimentary rocks. High Mg in the Buxton waters could also be derived in part from e.g. chlorite in a detrital aquifer. The low Ca and lack of Carboniferous evaporite inputs indicate a relatively short flow path within the limestone sequence. These lines of evidence imply that the Buxton thermal water has migrated from deep sandstone aquifers below the high ground to the west of Buxton before finally discharging through fissured limestone at the topographic low at the head of the Wye valley. Sandstones in these sequences are known to form relatively good aquifers (at least locally) with permeability largely through fracture systems. Individual boreholes in these sandstones typically yield 0.3 to 2.2 $l\,s^{-1}$ on pumping and some artesian wells in these sandstones below the Westphalian shales yield up to 4 $l\,s^{-1}$ under natural overflow conditions (Downing 1970). Thus, at Buxton the karstic permeability of the limestone (and possibly permeability associated with faulting at the limestone contact) is simply providing a hydraulically efficient pathway from the sandstone aquifer to a discharge point at a topographic low.

The Matlock-type waters have gained salinity by interaction with Lower Carboniferous evaporite deposits. The calculated depth of the thermal flow is consistent with the depth of buried evaporites in the sequence. The water chemistry and depth of flow do not require the thermal waters to have moved outside of the known Carboniferous Limestone sequence. Both thermal and non-thermal mine drainage waters on the eastern side of the White Peak show chemical and isotopic evidence for mixing of Matlock-type thermal water with shallow groundwater. The thermal risings at Matlock (including Meerbrook Sough) account for 97% of the groundwater thermal flux in the Dome (Edmunds

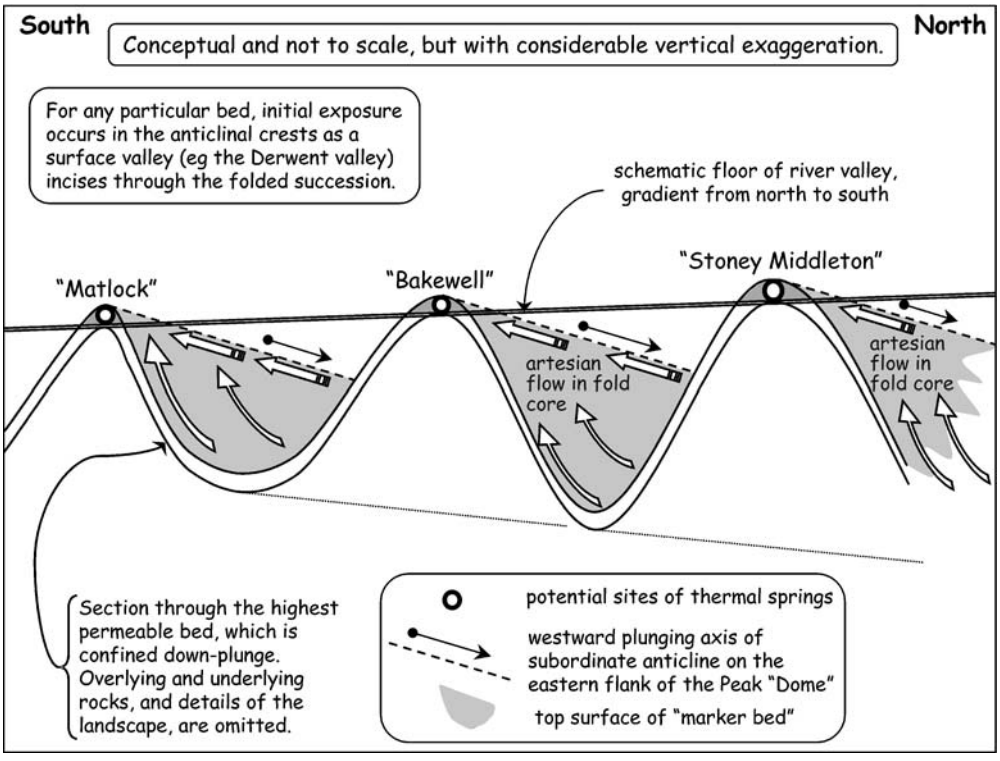

Fig. 10 Simplified structural geology of the Derwent valley and a conceptual model of its influence in focussing thermal spring flow into groups at the crests of antiforms, which form the lowest altitude outcrops of limestone

 DOI 10.1007/s10040-006-0022-7

1971) and these risings are grouped around the lowest altitude outcrop of limestone (Fig. 1). Along the eastern side of the main dome structure, thermal risings occur in groups where minor antiforms, trending approximately at right-angles to the dominant structural components of the Dome, have been truncated by the incision of the Derwent valley (Fig. 10). These provide 'targets' of lowest head in the aquifer toward which upward flow of thermal waters has been focussed. Figure 8 shows the clear effect of altitude of the rising on the flux of thermal water, the flux being concentrated at the lowest outcrop of the limestone.

As estimated above, the total discharge of Matlock-type thermal water is $\sim 15 \times 10^6$ m^3 year^{-1}. The precipitation excess over evapotranspiration in the area is 528 mm (MORECS square 106, 1961–1990 average value, Meteorological Office) and the Carboniferous Limestone catchment (including allogenic inputs) is $\sim$540 km^2, giving an annual recharge to groundwater of 285×10^6 m^3 year^{-1}. The discharge of thermal water is therefore $\sim$5% of the annual groundwater budget of the Carboniferous Limestone aquifer, requiring a recharge area of $\sim$29 km^2. These thermal waters have elevated sulphate concentrations due to evaporite dissolution which is occurring at rates likely to give rise to significant porosity and permeability enhancement in the deep aquifer. The development of deep high permeability flow paths is probably an essential prerequisite for the discharge of such large volumes of thermal water at surface.

Further evidence of deep groundwater flow in the White Peak Carboniferous Limestone aquifer comes from a negative temperature gradient between 450 and 575 m below ground level in the Eyam borehole, interpreted by Downing and Gray (1986) as being a consequence of deep groundwater movement. One of the authors (JG) has undertaken many water tracing experiments in the White Peak using fluorescent dyes, and these have determined the main flow paths of shallow groundwater in local flow systems. However, no tracer has been recovered at known springs from repeated injections in the Calton Hill area (Fig. 1) despite the use of very large amounts of dye. Hence, this area (and possibly other, as yet undetermined, areas) may be supplying recharge to long-term storage in the deep regional thermal flow system.

Conclusions

The Buxton and Matlock-type thermal waters exhibit chemical characteristics that testify to a high degree of water–rock interaction and long residence time, but otherwise have very different sources. A conceptual hydrogeological model for the waters is summarised in Fig. 9. The Buxton waters have a distinctive chemistry and are elevated in ^{87}Sr above limestone groundwaters. This implies an ultimate source in deeply-buried, locally confined, sandstone aquifers to the west of Buxton. The Matlock group of thermal risings (including Meerbrook Sough) account for 97% of the groundwater thermal flux in the White Peak (Edmunds 1971) and have interacted with evaporite deposits, confirming the deep underflow hypothesis of Worthington and Ford (1995). Importantly, there are similarities with the results of Krothe and Libra (1983) which suggest that this phenomenon is not unique to the White Peak and may be a widespread process in carbonate aquifers. Shallower groundwaters show no evidence of interaction with evaporites, deriving smaller amounts of sulphate instead by oxidation of sulphide minerals. Either evaporites were not present higher in the carbonate sequence, or these more soluble minerals were removed by similar deep groundwater flows when the land surface was higher. The present rate of dissolution of deep evaporites is significant and will give rise to zones of increased porosity and permeability deep within the aquifer. The presence of such zones would significantly influence later cavernous karst development by carbonic acid dissolution of limestone by providing an initial secondary porosity to allow the deep penetration of dissolutionally aggressive groundwaters. This supports the hypothesis of Lowe (2000) that processes not involving carbonate dissolution can be responsible for the inception of tertiary porosity and permeability (matrix = primary; fracture = secondary) in carbonate aquifers. Tertiary porosity/permeability is an essential precursor to the development of karstic drainage.

In the White Peak the discharge of the deep flow component is controlled regionally by the lowest outcrop of limestone in the Derwent valley. The discharge of Matlock-type thermal waters from mine adits results from the local lowering of groundwater head by driving of the adit and consequent upconing of the deeper thermal water. Deep regional thermal flow constitutes 5% of groundwater discharge from the Peak District limestone aquifer.

This study has demonstrated the power of combined isotopic studies of sulphate and strontium in distinguishing different sulphate sources and hydrogeological processes deep within a carbonate aquifer. It has also shown that deep evaporite dissolution can be a significant process on a regional scale in carbonate aquifers and give rise to early high permeability groundwater flow paths that influence later aquifer development by the 'normal' process of carbonate dissolution.

Acknowledgements This work was supported by NERC (Natural Environment Research Council) via an MSc studentship to Neil Webber at Leeds during the early part of this work. Later support was by a University of Huddersfield research studentship to Neil who collected water samples and undertook most of the laboratory analyses. Stable isotope facilities for groundwater studies were funded via NERC research grants GR3/7839 and GR3/8134 to SHB. We thank Bob Cliff of the University of Leeds for the Sr isotopic analyses and Rob Newton and Dave Hatfield for their expert assistance in the Leeds stable isotope lab. Critical and constructive comments by Tim Atkinson and Mike Edmunds have helped us to improve this work.

References

Aitkenhead N, Chisholm JI (1982) A standard nomenclature for the Dinantian formations of the Peak District of Derbyshire and Staffordshire. Report of the Institute of Geological Sciences, No. 82/8

 DOI 10.1007/s10040-006-0022-7

Aitkenhead N, Chisholm JI, Stevenson IP (1985) Geology of the country around Buxton, Leek and Bakewell. Memoir of the British Geological Survey, Sheet 111

Barker JA, Downing RA, Gray DA, Findlay J, Kellaway GA, Parker RH, Rollin KE (2000) Hydrogeothermal studies in the United Kingdom. Q J Eng Geol Hydrogeol 33:41–58

Bishop PK (1990) Precipitation of dissolved carbonate species from natural waters for $\delta^{13}C$ analysis—a critical appraisal. Chem Geol 80:251–259

Bishop PK, Lloyd JW (1990) Chemical and isotopic evidence for hydrochemical processes occurring in the Lincolnshire Limestone. J Hydrol 121:293–320

Bottrell SH, Novak M (1997) Sulphur isotopic study of two pristine *Sphagnum* bogs in the western British Isles. J Ecol 85:125–132

Bottrell SH, Webber N, Gunn J, Worthington SRH (2000) The geochemistry of sulphur in a mixed allogenic-autogenic karst catchment, Castleton, Derbyshire, UK. Earth Surf Process Landforms 25:155–165

Burke WH, Denison RE, Hetherington EA, Koepnick RB, Nelson HF, Otto JB (1982) Variation of seawater $^{87}Sr/^{86}Sr$ throughout Phanerozoic time. Geology 10:516–519

Chambers LA, Trudinger PA (1979) Microbiological fractionation of stable sulphur isotopes: a review and critique. Geomicrobiol J 3:249–293

Christopher NSJ, Wilcock JD (1981) Geochemical controls on the composition of limestone groundwaters with special reference to Derbyshire. Trans Brit Cave Res Assoc 8:135–158

Christopher NSJ, Beck JS, Mellors PT (1977) Hydrology—water in the limestone. In: Ford TD (ed) Limestones and caves of the Peak District, GeoAbstracts, Norwich, pp 185–230

Claypool GE, Holser WT, Kaplan IR, Sakai H, Zak I (1980) The age curves of sulfur and oxygen isotopes in marine sulfate and their mutual interpretation. Chem Geol 28:199–260

Cope FW (1973) Woo Dale Borehole near Buxton, Derbyshire. Nature 243:29–30

Cope FW (1979) The age of the volcanic rocks in the Woo Dale Borehole, Derbyshire. Geol Mag 116:319–320

Coulson JP, Bottrell SH, Lee JA (2005). Recreating atmospheric sulphur deposition histories from peat stratigraphy: Diagenetic conditions required for signal preservation and reconstruction of past sulphur deposition in the Derbyshire Peak District, UK

Crabtree RW, Trudgill ST (1984) Hydrochemical budgets for a Magnesian limestone catchment in lowland England. J Hydrol 74:67–79

Crowley SF, Bottrell SH, McCarthy MDB, Ward J, Young B (1997) $\delta^{34}S$ of Lower Carboniferous anhydrite, Cumbria and its implications for barite mineralization in the northern Pennines. J Geol Soc London 154:597–600

Downing RA (1967) The geochemistry of groundwater in the Carboniferous Limestone in Derbyshire and the East Midlands. Bull Geol Surv Great Britain No. 27, 289–307

Downing RA (1970) The hydrogeology of the Trent River basin. Water Supply Papers of the Institute of Geological Sciences, Hydrogeological Report No. 5. 104 pp

Downing RA, Gray DA (eds) (1986) Geothermal energy: The potential in the United Kingdom. HMSO, London

Dreybrodt W (1996) Principles of early development of karst conduits under natural and man-made conditions revealed by mathematical analysis of numerical models. Water Resou Res 32:2923–2935

Dunham KC (1973) A recent deep borehole near Eyam, Derbyshire. Nature 241:84–85

Edmunds WM (1971) Hydrogeochemistry of groundwaters in the Derbyshire Dome, with special reference to trace constituents. Report of the Institute of Geological Sciences, No.71/7

Edmunds WM, Smedley PL, Spiro B (1995). Controls on the geochemistry of sulphur in the East Midlands Triassic aquifer, UK. In: Isotopes in water resources management, vol. 2. Vienna, International Atomic Energy Agency, pp 107–122

Ewebank G, Manning DAC, Abbot GD (1995) The relationship between bitumens and mineralization in the South Pennine Orefield, central England. J Geol Soc London 152:751–765

Gabrovšek F, Dreybrodt W (2001) A model of the early evolution of karst aquifers in limestone in the dimensions of length and depth. J Hydrol 240:206–224

Gonfiantini R (1978) Standards for stable isotope measurements in natural compounds. Nature 271:534–536

Gonfiantini R (1984) Advisory group meeting on stable isotope reference standards for geochemical and hydrological investigations. Report of the Director General, IAEA. International Atomic Energy Agency, Vienna, 46 pp

Gunn J, Lowe DJ, Waltham AC (1998) The karst geomorphology and hydrogeology of Great Britain. In: Daoxian Y, Zaihua L (eds) Global karst correlation. VSP, The Netherlands, pp 109–135

Halas S, Shakur A, Krouse HR (1982) A modified method for SO_2 extraction from sulphates for isotopic analysis using $NaPO_3$. Isotopenpraxis 18:11–13

Hanna RB, Rajaram H (1998) Influence of aperture variability on dissolutional growth of fissures in karst formations. Water Resour Res 34:2843–2853

Institute of Geological Sciences (1978) IGS boreholes 1977. Report of the Institute of Geological Sciences, No.78/21

Krothe NC, Libra RD (1983) Sulfur isotopes and hydrochemical variations in spring waters of southern Indiana, USA. J Hydrol 61:267–283

Langmuir D (1971) The geochemistry of carbonate groundwaters in central Pennsylvania. Geochimica et Cosmochimica Acta 35:1023–1045

Lowe DJ (2000) Role of stratigraphic elements in speleogenesis: The speleoinception concept. In: Klimchouk AB, Ford DC, Palmer AN, Dreybrodt W (eds), Speleogenesis. Evolution of karst aquifers. National Speleological Society, Huntsville, Alabama, pp 65–76

McArdle NC, Liss PS (1996) Isotopes and atmospheric sulphur. Atmos Environ 29:2553–2556

McCarthy MDB, Newton RJ, Bottrell SH (1997) Oxygen isotopic compositions of sulphate from coals: implications for primary sulphate sources and secondary weathering processes. Fuel 77:677–682

McCrea JM (1950) On the isotope chemistry of carbonates and a palaeotemperature scale. J Chem Phys 18:849–857

Moncaster SJ, Bottrell SH, Tellam JH, Lloyd JW (1992) Sulphur isotope ratios as tracers of natural and anthropogenic sulphur in the Lincolnshire Limestone aquifer, eastern England. In: Kharaka Y, Maest AS (eds), Water-rock interaction. Balkema, Rotterdam, pp 813–816

Moncaster SJ, Bottrell SH, Tellam JH, Lloyd JW, Konhauser KO (2000) Migration and attenuation of agrochemical pollutants: insights from isotopic analysis of groundwater sulphate. J Contam Hydrol 43:147–163

Nicholson RV, Gillham RW, Reardon EJ (1988) Pyrite oxidation in carbonate-buffered solution: 1. Experimental kinetics. Geochimica et Cosmochimica Acta 52:1077–1085

Oxburgh ER, Richardson SW, Wright SM, Jones MGW, Penney SR, Watson SA, Bloomer JR (1980). Heat flow pattern in the United Kingdom. In: Strub AS, Ungemach P (eds), Advances in European geothermal research, Dordrect, Reidel, pp 447–455

Pentecost A (1999) The origin and development of the travertines and associated thermal waters at Matlock Bath, Derbyshire. Proc Geol Assoc 110:217–232

Robinson BW, Ineson PR (1979) Sulphur, oxygen and carbon isotope investigations of lead-zinc-barite-fluorite-calcite mineralization, Derbyshire, England. Trans Inst Min Metall 88:B107–B117

Smith K, Smith NJP, Holliday DW (1985) The deep structure of Derbyshire. Geol J 20:215–225

Strebel O, Bottcher J, Fritz P (1990) Use of isotope fractionation of sulfate-sulfur and sulfate-oxygen to assess bacterial desulfurication in a sandy aquifer. J Hydrol 121:155–172

Taylor SR (1983) A stable isotope study of the Mercia Mudstones (Keuper Marl) and associated sulphate horizons in the English Midlands. Sedimentology 30:11–31

 DOI 10.1007/s10040-006-0022-7

Tóth J (1963) A theoretical analysis of groundwater flow in small drainage basins. J Geophys Res 68:4795–4812

Turcotte DL, Schubert G (1982) Geodynamics. In: Applications of continuum physics to geological problems. Wiley, New York

Van Stempvoort DR, Krouse HR (1994). Controls of $\delta^{18}O$ in sulfate: review of experimental data and application to specific environments. In: Alpers CN, Blowes DW (eds), Environmental geochemistry of sulfide oxidation, American Chemical Society, Washington, DC, pp 446–480

Waters CN, Browne MAE, Dean MT, Powell JH (in press) BGS Lithostratigraphical framework for Carboniferous successions of Great Britain (Onshore). British Geological Survey Research Report, RR/05/06

Worthington SRH, Ford DC (1995) High sulfate concentrations in limestone springs: An important factor in conduit initiation? Environ Geol 25:9–15

Worthington SRH, Smart CC (2004) Groundwater in karst: conceptual models. In: Gunn J (ed), Encyclopedia of caves and karst science, Fitzroy Dearborn, London & New York, pp 399–401

 DOI 10.1007/s10040-006-0022-7